International Journal of Thermophysics, Vol. 17, No. 2, 1996

Molecular Simulation and Electron Paramagnetic Resonance (EPR) Studies of Rapid Bimolecular Reactions in Supercritical Fluids

S. Ganapathy,[1] T. W. Randolph,[2,3] C. Carlier,[2] and J. A. O'Brien[1]

Received March 20, 1995

We present comparisons among Brownian dynamics simulations, molecular dynamics simulations, and electron paramagnetic resonance spectroscopic studies of the Heisenberg spin-exchange reaction between nitroxide free radicals at near-infinite dilution in near-critical and supercritical ethane. We discuss the effects of correlations in the solute–solute and solvent–solute radial distribution functions on the rate constants for collision and reaction. We find that the enhancements in the local density of solvents around solutes strongly affect the rate constant for solvent–solute encounters. This result holds implications for those reactions where collisional-energy transfer from solvent to solute is the rate-limiting step. While the rate of collisions between solutes is strongly affected by solute–solute correlations for all densities, the reaction rate constant is affected by such local density augmentations only for certain combinations of density and collision lenght scale. Rate constants estimated computationally and experimentally show the same qualitative trend as a function of density. Collision lifetimes estimated from the simulations show a strong density dependence. These lifetimes reflect the competing effects of the intermolecular force and the potential of mean force and are distinctly bimodal at the higher densities.

KEY WORDS: Brownian dynamics; diffusion-controlled reactions; electron paramagnetic resonance spectroscopy; molecular dynamics; supercritical fluids.

[1] Department of Chemical Engineering, Yale University, New Haven, Connecticut 06520, U.S.A.

[2] Department of Chemical Engineering, University of Colorado, Boulder, Colorado 80309, U.S.A.

[3] To whom correspondence should be addressed.

0195-928X/96/0100-0471$09.50/0

1. INTRODUCTION

The choice of solvent is of vital importance in the rational design of any reaction system. The large compressibility of a supercritical fluid enables wide variation in solvation with modest changes in temperature and pressure. This has spurred the study of reactions in supercritical fluids. However, there is a lack of the fundamental understanding of the solvent effects of supercritical fluids on chemical reactions.

The molecular structure of supercritical fluid mixtures has received much recent attention. Specifically, there has been a focus on the phenomenon of local density augmentation of solvent molecules around solute molecules present at near-infinite dilution and of local density augmentation of solutes around other solute molecules. Several spectroscopies (UV[1, 2], photo ionization [3, 4], fluorescence [5, 6], and EPR [7]) have shown that such local density effects exist. Further evidence has been provided by integral equation theory [8, 9] and molecular dynamics simulations [10] of supercritical fluid systems.

Such solvent–solute and solute–solute excesses could be expected to influence reaction rates, yet experiments do not always show this to be the case. Both solvent–solute and solute–solute local density enhancement effects have been observed in some, but not all, reaction studies to date [11–16]. We have attempted to provide a microscopic understanding of the effect of local densities (both solvent–solute and solute–solute) on rapid bimolecular reactions by comparing molecular dynamics and Brownian dynamics simulations of an infinitely fast reaction that models Heisenberg spin-exchange and electron paramagnetic resonance (EPR) spectroscopic studies of the same reaction.

2. METHODOLOGY AND BACKGROUND

Heisenberg spin-exchange is a rapid bimolecular reaction in which radicals possessing opposite spin states exchange spins by colliding with each other. More details of this reaction can be found elsewhere [17]. In our group, EPR studies of spin-exchange between di-butyl nitroxide (DTBN) radicals in near-critical and supercritical ethane have been carried out [18]. In our simulations, both DTBN and ethane were approximated as spherical molecules each possessing Lennard–Jones (L-J) size and energy parameters σ and ε, respectively. O'Brien and co-workers have estimated the L-J parameters for DTBN [19], while the L-J parameters of ethane are readily available in the literature [20].

NVE molecular dynamics (MD) and equilibrium Brownian dynamics (BD) simulations of DTBN in ethane were carried out over a wide range

of densities. Details of these simulations are given elsewhere [19, 21]. All parameters were made dimensionless using solute L-J parameters [22]. All simulations were carried out at a reduced temperature of $T_r = 1.084$ (which corresponds to a dimensionless temperature $T^* = 0.6336$ in solute L-J units). Note that the simulations were carried out at near-infinite dilution of the solute (mole fractions between 10^{-2} and 10^{-3}). Hence, the critical temperature and critical density used for computing reduced variables are those of the pure Lennard–Jones solvent [23], which in solute L-J units are $T^*_{C,LJ} = 0.5846$ and $\rho^*_{C,LJ} = 1.6375$.

The essence of the Brownian dynamics technique lies in representing the solvent as an effective viscosity field, i.e., neglecting solvent structure. Therefore, the choice of an effective simulation box length is completely independent of solvent critical fluctuation lengths. The solute diffusivities that are input to BD simulations must, however, be picked carefully. We precomputed these diffusivities in long MD runs. In *these* MD runs, care was taken to ensure that the simulation box lengths at near-critical conditions were considerably larger than the pure solvent correlation length

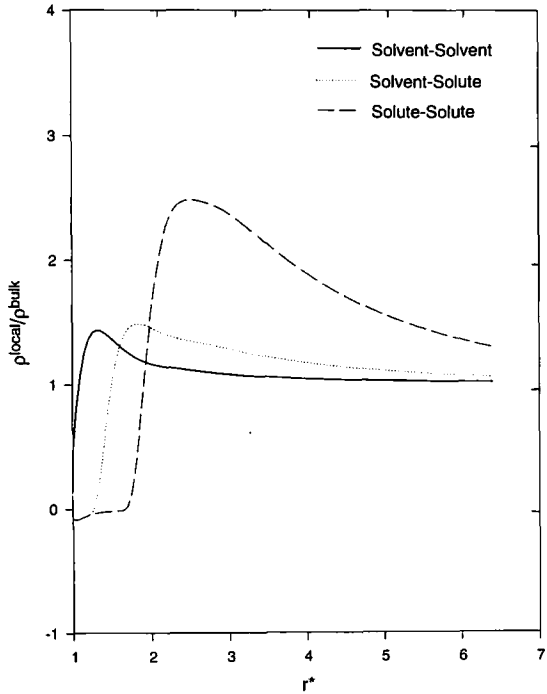

Fig. 1. Local to bulk density ratio vs r^* calculated from Eq. (1) and the Ornstein–Zernike integral equation.

[19]. This ensured that diffusivities from these simulations were essentially unaffected by critical density fluctuations.

The local density in a fluid can be estimated in the following fashion:

$$\frac{\rho^{\text{local}}(r)}{\rho^{\text{bulk}}} = 1 + \frac{3\int_{r_{\min}}^{r} r^2[\,g(r)-1\,]\,dr}{(r^3 - r_{\min}^3)} \tag{1}$$

Here $r_{\min}$ is the separation distance where the radial distribution function $g(r)$ becomes significantly nonzero, usually at about $r^* = 0.9$.

Local solvent–solvent, solute–solvent, and solute–solute density enhancements estimated by applying the Percus–Yevick closure to the Ornstein–Zernike equation [24] at a reduced density of $\rho_r = 0.6$ are illustrated in Fig. 1. There is significant enhancement for all three cases, but the solute–solute enhancement is the largest. Also, the local density enhancement is largest at a value of r^* not much different from the solute L-J radius, suggesting that such enhancements should significantly affect the rate of those reactions whose cybotactic length scale is comparable to the van der Waals radius of the reactants.

3. RESULTS

In our simulations, we considered the case of a reaction with infinitely fast kinetics in which every collision results in reaction. We probed the influence of solvent–solute clustering on the rate of solvent–solute collisions in a nonreacting environment. Solute–solute local density effects on collision and reaction rate constants were studied. In addition, we measured the lifetime of collisions between solutes over a wide density range. In our simulations, we have defined a collision as occurring when two colliding molecules reach a specified distance R_c^* from each other. By varying this encounter distance, we have estimated quantities of interest both as a function on density and of collision length scale.

3.1. Solvent–Solute Local Density Effects

The rate constant for bimolecular collisions from kinetic theory [25] is given by [21, 26, 27]:

$$(k_{\text{col}}^*)_{ij} = 2\pi(R_c^*)^2 \left(\frac{2T^*}{\pi}\right)^{0.5} \left(\frac{m_i}{m_j} + 1\right)^{0.5} g_{ij}(r)\Big|_{R_c^*} \tag{2}$$

where $(k_{\text{col}}^*)_{ij}$ is the dimensionless rate constant for collisions, R_c^* is the dimensionless collision length scale, and $g_{ij}(r)/_{R_c^*}$ This result was derived

for solute–solute collisions in a structureless solvent. We attempted to show that Eq. (2) holds for solvent–solute collisions as well, in the following fashion. The rate constant for solvent–solute collisions was normalized by $2(R_c^*)^2(2T^*\pi)^{0.5}(1+m_i/m_j)^{0.5}$ and was plotted as a function of the collision radius for three different densities as shown in Fig. 2. It can be seen that this ratio is quantitatively equal to the solute–solvent radial distribution function $g_{12}(r)$. Thus, for collision length scales not very different from the Van der Waals radius, the rate of solvent–solute collisions is strongly influenced by the local solvent density. For large collision radii, however, the radial distribution function decays to unity and the collision rate is unaffected by local density effects.

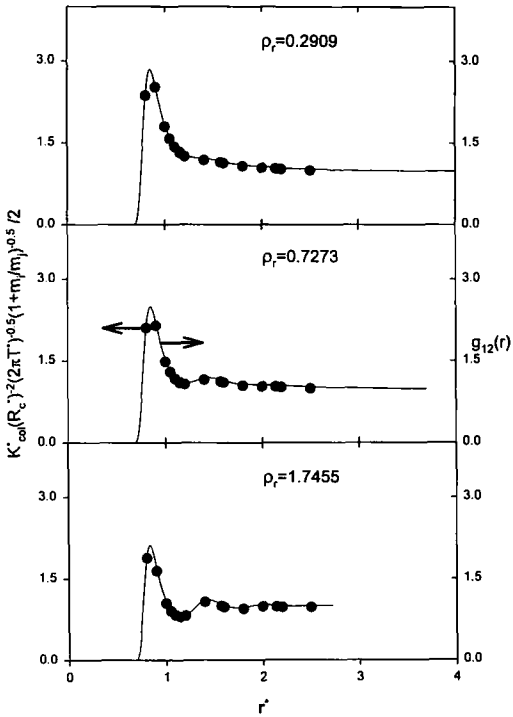

Fig. 2. The effect of collision length scale r^* (non-dimensionalized in solute L-J units) on the normalized solvent–solute collision rate constant. The line is $g_{12}(r)$ obtained from the same simulation runs, while the filled circles represent the rate constants. There is exact quantitative agreement for all three densities shown.

3.2. Solute–Solute Local Density Effects

BD simulations were carried out to estimate reaction rate constants. An isotopic reaction scheme was used [27] in which a statistical concentration gradient was created by preventing molecules that have reacted from reacting again. For such diffusion–limited reactions, the Smoluchowski theory predicts the reaction rate constant as [28]:

$$k^*_{\text{react}} = 4\pi R_c^* D^* \tag{3}$$

where R_c^* is the sum of the collision radii and D^* is the sum of the diffusion coefficients of the two reactants.

Reaction rate constants were estimated as a function of density and collision radius. To test the radial dependence of the reaction rate, the rate constant normalized by the modified kinetic theory result of Eq. (2) is plotted against the collision radius as shown in Fig. 3. Also plotted is the rate constant from Smoluchowski theory normalized by Eq. (2). At the

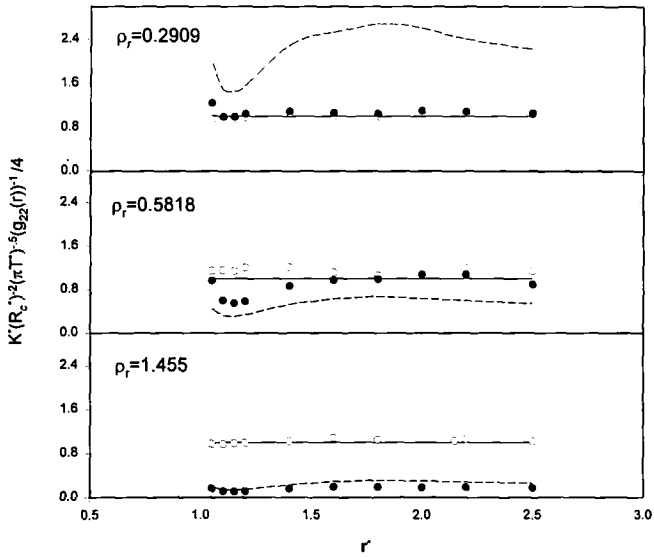

Fig. 3. Comparison of the effect of collision length scale r^* on the solute–solute collision rate constants and reaction rate constants. All of the rate constants have been normalized by the modified kinetic theory result of Eq. (2). Also shown by dashed lines is the Smoluchowski limit modified by Eq. (2). The open circles represent the collision rate constants and the closed circles represent the reaction rate constants. The solid line shown represents the modified kinetic theory prediction. These comparisons are shown over three densities.

lowest density, the normalized reaction rate constant falls on the line from kinetic theory predictions. At the intermediate density, it differs from the values both from kinetic theory and from the Smoluchowski theory, while at the highest density, it is well predicted by the Smoluchowski theory. This is reasonable since at high densities, the equilibrium radial distribution function (RDF) for the unreacted molecules (i.e., those still available for reaction) is determined by the combination of reaction and diffusive transport limitation. Despite this, the equilibrium RDF for all the reacted and unreacted solute molecules taken together is still the original equilibrium RDF. The high density result for the unreacted molecules shows little or no short-range structure and, hence, the reaction rate shows no local structural effects. At the low densities however, the time scale required for reaction is large compared to the time required for the fluid to relax into its equilibrium structure and hence the effect of $g_{22}(r)$ is clearly seen.

However, no such variations are seen for the rate constants for solute–solute *collisions*, which are also shown in Fig. 3 normalized by Eq. (2). As can be seen, these collision rate constants are exactly predicted from the modified kinetic theory over all density ranges. Collision rates are always influenced by the equilibrium solute–solute radial distribution function $g_{22}(r)$ since nonreactive collisions do not influence the equilibrium structure of the fluid.

3.3. Comparison with EPR Measurements

The materials and methods used to carry out EPR spectroscopic measurements of spin-exchange are described elsewhere [18]. Reaction rate constants measured as a function of density from the BD simulations for a collision radius of $r = 1.0\ \sigma_{22}$ are plotted alongside the rate constants from EPR as shown in Fig. 4. It can be seen that the rate constants from experiments and simulations qualitatively resemble each other, in that they exhibit the same density dependence in the limiting regimes of reaction behaviour (plateau at low density, linear with inverse density at high density). To provide a quantitative comparision, two quantities are needed: (a) the cybotactic radius for spin-exchange and (b) the reaction probability. The cybotactic length scale for spin-exchange is estimated to be between one and three hard-sphere diameters [29]. The reaction probability is a function of the lifetime of collisions between reactants, with an upper bound of one-half [18]. Note that the computationally determined rate constants assume a reaction probability of unity.

One of the keys to understanding solvent structural effects on reactions is to know what the real collision length scale required for reaction

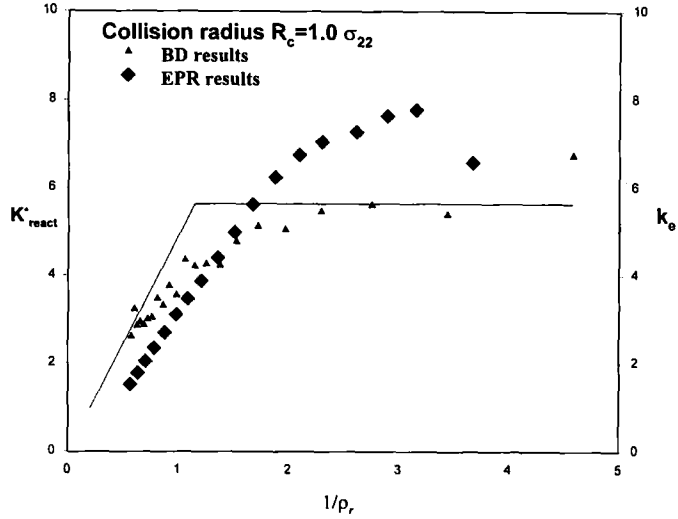

Fig. 4. Comparison of the reaction rate constants from BD simulations and EPR studies as a function of $1/\rho_r$. The BD results are for a collision radius of $r = 1.0\sigma_{22}$. The horizontal line represents the kinetic theory result of Eq. (2), while the skewed line corresponds to the Smoluchowski prediction of Eq. (3). EPR results have been scaled by a factor of two; this factor is the lower bound on probability effects on the Heisenberg spin-exchange reaction.

is. Quite obviously, different reactions have different collision length scales; based on our results therefore, the effect of local densities on different reactions is different. To predict and understand the kinetic effects of solvents by comparing and contrasting the various experimental studies of reactions, it is essential to have precise quantitative estimates of the collision length scale required for all of the reaction systems being studied.

3.4. Collision Lifetimes

We measured the lifetimes of individual solute–solute collisions in BD simulations over the density range from $\rho_r = 0.1455$ to $\rho_r = 1.455$ for a collision radius of $r = 1.57\sigma_{22}$. Collision lifetime distributions obtained, as shown in Fig. 5, are strongly density dependent. At the intermediate densities the lifetime are distinctly bimodal. Note that the distributions have been normalized such that the integral of each distribution is unity.

For the purpose of illustration, we have marked as "A" and "B" the two peaks that appear in the lifetime distributions. At the lower densities,

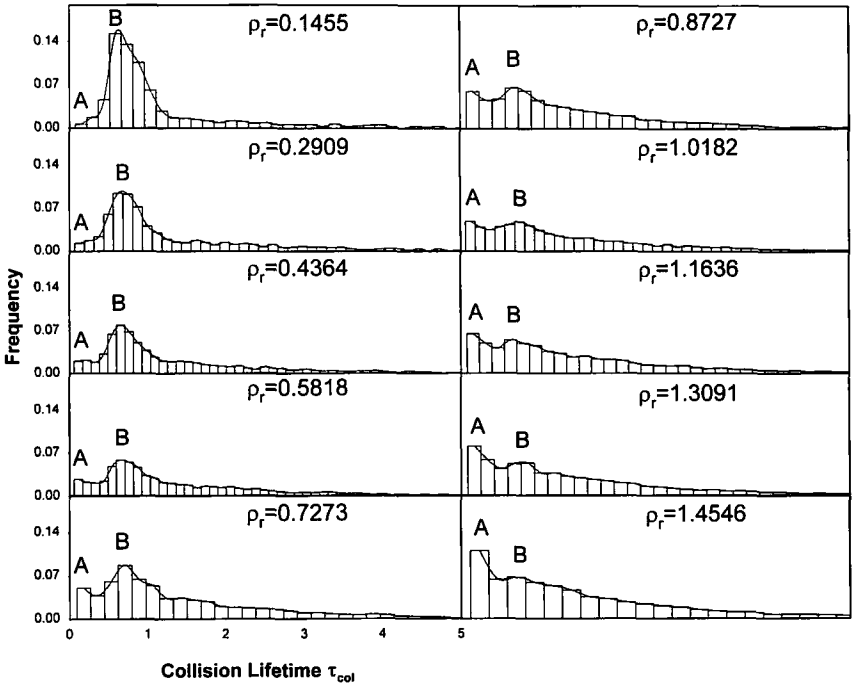

Fig. 5. A plot of the collision lifetime distributions over the density range of $\rho_r = 0.1455$ to $\rho_r = 1.455$. The ordinate represents the frequency of the collision lifetimes, while the abscissa denotes the collision lifetime τ_{coll} (in solute L-J units). All distributions are plotted on the same scale. These lifetimes were estimated for a collision radius of $r = 1.57\sigma_{22}$. Interestingly, most of the density space where the lifetime distributions are distinctly bimodal falls in the near- and supercritical region for this collision length scale.

peak B is very prominent, while at the higher densities, it all but disappears and peak A is dominant. At the low densities, when molecules move thermally rather than diffusively, the tendency to sit in each other's potential well is very strong since the effect of the mean field is small. Most collisions that occur at these densities are mediated by the intermolecular interaction, and this causes the single peak B in the lifetimes. This result is consistent with observations of gas-phase clustering which predict such trends in the collision lifetime [30].

At the higher densities, however, it is the potential of mean force that is significant. This increases the duration of collisions. It can be seen from Fig. 5 that the lifetime distributions at high densities exhibit long tails. Our observations are consistent with the first passage time results for estimating average survival lifetimes in diffusive processes [31]. If we consider that

$\Sigma(t)$ denotes the survival probability and the mean time for diffusion is given by the Einstein relation [32], we can write [33]

$$\Sigma(t) = \exp(-6Dt/R_c^2) \tag{4}$$

Equation (4) represents an exponential decay of the survival probability distribution with time. Hence, peak A is qualitatively predicted from this relation. For small values of the diffusivity (*i.e.* high densities), the probability distribution is significantly nonzero even at long times.

The lifetime distributions may thus be thought to reflect the counteracting influences of the intermolecular potential and the potential of mean force. While the low-density and high-density effects on collision lifetime are understood, the bimodel behavior that occurs at the intermediate densities is not. The occurrence of the bimodal region is due to the fact that neither the intermolecular force nor the potential of mean force clearly dominates at the intermediate densities. It is interesting to note that for reactions requiring collision length scales that are not much larger than the hard-sphere value, the density range where this bimodal behavior occurs falls in the near- and supercritical region.

4. CONCLUSION

The rate of solute–solvent collisions has been shown to be directly related to the radial distribution function $g_{12}(r)$. Even though this treatment was for transport-limited reactions, this result has implications for those reactions where the rate-determining step is collisional–energy transfer between solvent and reactant [34]. It has also been shown that correlations in the radial distribution function $g_{22}(r)$ strongly affect solute–solute collision rates. They affect reactions rates only at the lower densities and for certain collision radii. We have also compared our rate constants from BD simulations with EPR spectroscopic measurements; the two sets of rate constants display the same qualitative trend as a function of density. Collision lifetimes estimated from the simulations display a strong density dependence. They are distinctly bimodal at the higher densities and reflect the competing effects of the intermolecular force and the potential of mean force.

ACKNOWLEDGMENTS

Acknowledgment is made to the National Science Foundation for its support through the Presidential Young Investigator Award and Grant CTS 9414759 to T.W.R. and Grant CBT-8809548 to J.O.'B. The authors

thank Professor Peter Monson for the computer program used for Ornstein–Zernike equation calculations.

REFERENCES

1. S. Kim and K. P. Johnston, *Ind. Eng. Chem. Res.* **26**:1206 (1987).
2. C. R. Yonker and R. D. Smith, *J. Phys. Chem.* **92**:235 (1988).
3. K. Nakagawa, A. Ejiri, K. Kimura, and M. Nishikawa, *Phys. Scripta* **41**:140 (1990).
4. K. Nakagawa, *Radiat. Phys. Chem.* **37**:643 (1991).
5. J. F. Brennecke, D. L. Tomasko, J. Peshkin, and C. A. Eckert, *Ind. Eng. Chem. Res.* **29**:1682 (1990).
6. Y.-P. Sun, M. A. Fox, and K. P. Johnston, *J. Am. Chem. Soc.* **114**:1187 (1992).
7. C. Carlier and T. W. Randolph, *AIChE J.* **39**:876 (1993).
8. H. D. Cochran and L. L. Lee, *ACS Symp. Ser.* **448**:60 (1992).
9. P. G. Debenedetti., *Chem. Eng. Sci.* **42**:2203 (1987).
10. B. L. Knutson, D. L. Tomasko, C. A. Eckert, P. G. Debenedetti, and A. A. Chialvo, in *Supercritical Fluid Technology*, F. V. Bright and M. E. P. McNally, eds., *ACS Symp. Ser.* **448**:60 (1992).
11. K. P. Johnston and C. Hayes, *AIChE J.* **33**:2017 (1987).
12. J. E. Chateauneuf, C. B. Roberts, and J. F. Brennecke, in *Supercritical Fluid Technology*, F. V. Bright and M. E. P. McNally, eds., *ACS Symp. Ser.* **448**:48 (1992).
13. J. Zagrobelny and F. V. Bright, *J. Am. Chem. Soc.* **114**:7821 (1992).
14. C. B. Roberts, Z. Zhang, J. F. Brennecke, and J. E. Chateauneuf, *J. Phys. Chem.* **97**:5618 (1993).
15. B. Otto, J. Schroeder, and J. Troe, *J. Chem. Phys.* **81**:202 (1984).
16. J. R. Combes, K. P. Johnston, K. E. O'Shea, and M. A. Fox, *Supercritical Fluid Technology*, F. V. Bright and M. E. P. McNally, in *ACS Symp. Ser.* **448**:31 (1992).
17. Y. N. Molin, K. M. Salikhov, and K. I. Zamaraev, *Spin Exchange Principles and Applications in Chemistry and Biology* (Springer Verlag, New York, 1980).
18 T. W. Randolph and C. Carlier, *J. Phys. Chem.* **96**:5146 (1992).
19. J. A. O'Brien, T. W. Randolph, C. Carlier, and S. Ganapathy, *AIChE J.* **39**:1061 (1993).
20. J. M. Prausnitz, *Molecular Thermodynamics of Fluid Phase Equilibra* (Prentice-Hall, Englewood Cliffs, NJ, 1969), p. 107.
21. S. Ganapathy, T. W. Randolph, and J. A. O'Brien, *AIChE J.*, in press (1995).
22. M. P. Allen and D. J. Tildesley, *Computer Simulation of Liquids* (Oxford University Press, New York, 1987).
23. B. Smit, P. De Smedt, and D. Frenkel, *Mol. Phys.* **68**:931 (1989).
24. D. B. McGuigan and P. A. Monson, *Fluid Phase Equil.* **57**:227 (1990).
25. J. O. Hirschfelder, C. F. Curtiss, and R. B. Bird, *Molecular Theory of Gases and Liquids* (Wiley, New York, 1954).
26. S. Chapman and T. G. Cowling, *The Mathematical Theory of Non-Uniform Gases* (Cambridge University Press, Cambridge, U.K., 1970).
27. T. W. Randolph, J. A. O'Brien, and S. Ganapathy, *J. Phys. Chem.* **98**:4173 (1994).
28. M. V. Z. Smoluchowski, *Phys. Chem.* **92**:129 (1917).
29. D. M. Bartels, A. D. Trifuac, and R. G. Lawler, *Chem. Phys. Lett.* **152**:109 (1988).
30. D. L. Bunker, *J. Chem. Phys.* **32**:1001 (1960).
31. N. Agmon, *J. Chem. Phys.* **81**:3644 (1984).
32. S. Chandrasekhar, *Rev. Mod. Phys.* **15**:1 (1943).
33. A. Szabo, K. Schulten, and Z. Schulten, *J. Chem. Phys.* **72**:4350 (1980).
34. A. G. Zawadzki and J. T. Hynes, *J. Phys. Chem.* **93**:7031 (1989).